



Scalable continuous solvothermal synthesis of metal organic framework (MOF-5) crystals

Colin McKinstry^{a,b}, Russell J. Cathcart^a, Edmund J. Cussen^{b,*}, Ashleigh J. Fletcher^a, Siddharth V. Patwardhan^{a,*}, Jan Sefcik^a

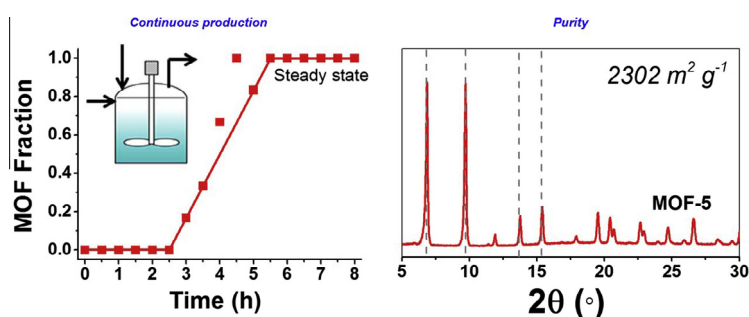
^a Department of Chemical and Process Engineering, University of Strathclyde, 75 Montrose Street, Glasgow G1 1XJ, UK

^b WESTCHEM, Department of Pure and Applied Chemistry, University of Strathclyde, 295 Cathedral Street, Glasgow G1 1XL, UK

HIGHLIGHTS

- Pure MOF manufactured in a continuous process with a high space time yield.
- Compared common solvents to explore economically viable industrial manufacturing.
- Optimised the process in order to produce high purity, high surface area MOF-5.

GRAPHICAL ABSTRACT



ARTICLE INFO

Article history:

Received 8 May 2015

Received in revised form 2 October 2015

Accepted 6 October 2015

Available online 22 October 2015

Keywords:

Manufacturing

Microporous materials

Zn₄O(BDC)₃

ABSTRACT

Metal–organic frameworks (MOFs) are well suited as nanoporous materials for applications such as gas storage, catalysis and in medical devices. Literature predominantly covers information on the batch synthesis of MOF-5, however, for an industrially viable product to be formed, bridging the gap to scalable continuous processing is essential. Here, we show that crystals of MOF-5 can be formed in a scalable solvothermal continuous process with a maximum space time yield of nearly 1000 kg m⁻³ day⁻¹. Analysis of the solid output as a function of time, in conjunction with variation of concentration of the feed supply, shows high purity MOF-5 is produced using a continuous system, with potentially high throughput on scale up. We also show that the output can be increased by increasing the concentration of reactants in the system, albeit resulting in a reduced surface area. The two most common solvents currently used for MOF-5 production are also compared to identify a more economically viable process.

© 2015 The Authors. Published by Elsevier B.V. This is an open access article under the CC BY license (<http://creativecommons.org/licenses/by/4.0/>).

1. Introduction

Metal–organic framework (MOF) materials [1] are of considerable interest due to the unique properties granted by the nature of their supramolecular construction [2,3]. This method of material design allows MOFs to be potentially tailored in aspects such as

pore size and bonding strength by careful choice of the metal ion centre [4] and ligand group [5] used. Ligands with side-chains can be used to allow further functionality to the material, allowing for the possibility of a truly tunable system at the molecular level [6]. The ability of three-dimensional MOFs to form scaffold-like structures reduces the dead space within a bulk volume to almost zero, providing considerable benefits to gas processing using MOFs. Their tailored syntheses has allowed several MOFs to have surface areas larger than that deemed possible in carbon structures or

* Corresponding authors.

E-mail addresses: Edmund.Cussen@strath.ac.uk (E.J. Cussen), Siddharth.Patwardhan@strath.ac.uk (S.V. Patwardhan).

zeolites [6]. As such, MOFs have great potential in gas storage and separation processes, catalysis and use in medical devices.

However, as most procedures for MOF synthesis are small-scale batch processes, only rare studies report production on the order of kg scale [7]. Many MOF syntheses require expensive ligands or the use of costly and non-reusable solvents. MOF syntheses are reported in the literature to be via wide variety of batch routes, including solvothermal [8], ultrasonic enhanced [9], microwave heated [10], diffusion or direct addition of amines [11] and growth on substrates [12]. Solvothermal synthesis is the most commonly applied synthetic route, allowing the system to be operated without the need for specialist equipment and the relatively fast growth of crystals with high levels of crystallinity, phase purity and surface areas [13]. While synthetic techniques, including mechanochemical synthesis, can reduce solvent usage significantly when producing MOFs with high yields, such routes incur heat transfer issues and high mechanical energy requirements on scale up that may limit applications [14]. Although this route has shown promise with scalability for some MOFs, it has been highlighted that this route is dependent on the ability of the MOF to withstand the mechanical and thermal strains of mechanochemical synthesis [15] and hence it is not suitable for all MOFs.

The high synthetic costs of MOFs have impeded the development of viable industrial uses; for MOFs to be economically viable, a reduction in the unit cost via scale-up, and switching from batch to continuous processing, is required, which has been confirmed by our preliminary process economics analysis [16]. Continuous methods offer several benefits compared to more traditional batch systems that are used to produce MOFs at the current time, such as higher output per unit time and, theoretically, zero downtime. Furthermore, when a reactor reaches steady state, the product output from the system is consistent, and eliminates variability that would be seen between batches. The capital cost and design complexity of continuous processing is increased compared to batch systems but the benefits in output can outweigh this issue, allowing greater economic viability [17].

Microfluidic reactors have been used, and with promising results for many materials, including HKUST-1, MOF-5 and MIL-53, three prototypical MOFs. Microfluidic reactions rely upon formation of nanoliter scale droplets which results in efficient heat and mass transfer, while also providing a very high surface area to volume ratio [18]. MOF-5 has been synthesised using a continuous microfluidic reactor, resulting in the formation of MOF-5 in 3 min at 120 °C, a significant reduction in reaction duration at this temperature, and BET surface area of 3185 m² g⁻¹. IRMOF-3, with different composition but the same topology as MOF-5 was also synthesised in similar times. UiO-66 was shown to be synthesised in 15 min at 140 °C using the same approach [18]. However, microfluidic syntheses are not necessarily scalable since transport properties scale non-linearly with production scales [19,20]. In terms of scalability, microfluidic systems rely upon the very high surface area to volume ratios and the heat transfer and mass transfer of single droplets of reaction solution, usually under 200 µm in diameter, in oil. While control over these droplets can increase throughput, the current upper limit appears to be in the order of hundreds of ml h⁻¹ [21] and so scalability may be an issue despite the benefits of using microfluidics.

Recent advances have shown it is possible to produce UiO-66-NH₂ in a scalable reaction system [22]. HKUST-1, previously produced using the microfluidic approach has also shown promise at larger scales of continuous processing. Gimeno-Fabra et al. [23] showed the ability to form high quality HKUST-1 using a counter-current flow reactor operating at 300 °C and 250 bar, bringing the required synthesis time for HKUST-1 from hours by conventional synthesis to 1 s while maintaining a high surface area. Kim et al. [18] reported continuous production of HKUST-1,

showing the capability of producing high yields of high quality crystals in reaction times as short as 5 min with considerably less harsh operating conditions than Gimeno-Fabra et al., though still operating at 100 bar. Rubio-Martinez et al. [24] reported the ability to make HKUST-1, UiO-66 and NOTT-400 in a continuous process and demonstrated the ability to scale the reaction volume of HKUST-1 from 10 ml to 108 ml while maintaining the high surface area of the MOF, with higher reported surface area than Kim et al. Further, this system operates at pressures relatively close to atmospheric conditions, reducing the intrinsic risk of the process. Bayliss et al. synthesised MIL-53 in a potentially scalable system, showing a reduction in synthetic duration from the order of days to minutes, with surface area consistent with prior literature though significantly, pressure of 100 bar was used for this system [25]. Increasing the temperature and pressure for MOF synthesis has been shown to provide thermodynamic conditions that result in the formation of the framework in considerably shorter times than previously reported in the literature [26], however operating at elevated temperatures and pressures is likely to increase the overall cost of the process significantly.

In this study, we focus on production of MOF-5, which has the composition Zn₄O(BDC)₃ (BDC = benzene dicarboxylate anion) [27]. MOF-5 has been a material of great interest in the scientific literature due to the high surface area, since the structure was first published in 1999. Although they have been recently surpassed in some key criteria by other MOFs, the zinc-carboxylate MOFs represent a large family of isorecticular structures which are anticipated to have useful applications in the future. Further, despite continuous syntheses reported at small scales, there are no reports on the large-scale production of MOF-5. Therefore, we selected MOF-5 as a model system, and developed a continuous process for its synthesis, which could facilitate the development of continuous manufacturing processes for other IRMOF compounds. While continuous MOF-5 production has been shown using microfluidic reactions [18], no scalable system has been published for this MOF. The batch conditions affecting MOF-5 synthesis are mainly treatment time, temperature, concentration and solvent. MOF-5, like many other MOFs, is known to form interpenetrated structures when the concentration exceeds a critical point. Such interpenetration results in the formation of a second network interwoven through the free space of the parent framework, thus greatly reducing the internal volume accessible and adversely affecting the desirable properties of the MOF. Therefore, it is challenging to strike a balance between solvent reduction and maximising cost efficiency by increasing solid throughput, while maintaining the quality of the MOF. The choice of solvent is crucial when considering the economics of large scale production of MOF-5 that exhibits desirable properties. MOF-5 is generally formed by using either *N,N*-diethylformamide (DEF) or *N,N*-dimethylformamide (DMF) [6] as the synthetic solvent. The use of DEF has been shown to form products with higher surface areas (average ~3200 m² g⁻¹ for DEF vs. ~2200 m² g⁻¹ for DMF, although values reported vary greatly), but DEF is considerably more expensive than DMF, usually by a factor of 6–10 times. Analysis of solvent choices for continuous production systems allows process viability to be determined via an informed compromise between cost and surface area. The space-time yield (STY) is a significant metric and allows a direct comparison of the dry yield of a system, normalised with respect to time and reactor volume. The core aims of this work include creating an efficient and scalable system, increasing the STY of the product without significantly impacting the quality of the crystalline product, and attempting to keep costs low by operating at less harsh conditions.

This work presents a reactor system that can produce MOF-5 in a continuous process, using a stirred tank reactor (CSTR) operating at atmospheric pressure. Important objectives of this study are to

optimise the efficiency of MOF-5 synthesis by varying residence time, to intensify production via increased concentration and to compare the two main solvents used for MOF-5 synthesis, presenting a wider overview of the key parameters affecting continuous MOF-5 production. Due to the potential added costs at industrial scale of operating at high pressures, we elected to probe operation at atmospheric pressure. The product quality was assessed through crystallinity and specific surface area, measured using powder X-ray diffraction (PXRD) and nitrogen adsorption, respectively. Understanding of the effects of synthesis parameters on MOF-5 product quality gained here will be of value in development of continuous large-scale manufacture of MOFs.

2. Experimental

2.1. Continuous synthesis of MOF-5

The experimental layout of the system was split into 3 sections: feed, reactor and collection (Fig. 1 and S1). The feed section comprised terephthalic acid (H_2BDC) solution in a reflux condenser and a separate solution of zinc nitrate in a conical flask. Both solutions require stirring to achieve complete dissolution. At low concentrations, H_2BDC will completely dissolve at ambient conditions, however, at the higher end of the range of concentrations investigated, significant heating ($T = 100\text{ }^\circ\text{C}$) was required, hence, a reflux condenser was used to minimise solvent losses. Calibrated peristaltic pumps (Watson Marlow 101-U) with a combination of silicone and PTFE tubing were used to feed the reactor from the bulk feed solutions described above. The reactor itself was run under reflux due to the boiling point depression caused, for both solvents, by the presence of the reactants and the reaction temperature being close to the solvent boiling points. The reaction and feed solution temperatures were monitored *in situ* by either a thermometer or a thermocouple placed into the solution. The feed tubes were allowed to drip feed into the reactor from slightly above the solvent level. PTFE tubing was used to remove the product from the bottom of the reactor. To enable product collection, another peristaltic pump was used to pump the product suspension into a new, disposable, glass vial. Samples were collected for 20–30 min periods and allowed to cool to room temperature before being vacuum dried and stored under vacuum prior to any further analysis.

The solvents used were *N,N*-diethylformamide (DEF) (SAFC, 99%) and *N,N*-dimethylformamide (DMF) (Sigma Aldrich, 99.8%, anhydrous). Each experiment used only one solvent for both continuous feeds and the initial reactor feed. The synthetic conditions were similar to those reported for a batch system reported in our previous work [28]. Briefly, the feed supply consisted of 0.314 g zinc nitrate tetrahydrate (Emsure $\geq 98.5\%$) dissolved in 100 ml solvent and 0.0666 g terephthalic acid (Alfa Aesar 98%) dissolved

in a second container of 100 ml solvent. The initial reactor mixture consisted of 100 ml solvent. This solution was heated to the reaction temperature before 0.157 g zinc nitrate tetrahydrate and 0.0333 g terephthalic acid (H_2BDC) were added as the pumps were switched on resulting in a Zn:BDC: H_2O ratio of 3:1:12. The feed solutions were mixed when entering the reactor to maintain the reactor concentration throughout the experiment. The precursor feed concentrations were increased for process intensification such that the 100% theoretical yield in grams varied between 1, 3, 5 and 10 g per 100 ml reactor output (i.e. 1%, 3%, 5% and 10% solids) while temperature was maintained at $140\text{ }^\circ\text{C}$ throughout. We further compared the effect of Zn:BDC ratio by investigating the stoichiometric ratio of zinc and BDC of 4:3 (stoichiometric) by changing feed concentrations, while keeping the flowrates unchanged.

As the solvent was heated to the reaction temperature before the pumps were started or precursors were added to the reactor vessel, the time at which the pumps were turned on was, therefore, noted as $t = 0$ for these experiments. In initial experiments, the pumps were set to 50 ml h^{-1} flow rates, giving a residence time of 2 h. Residence times were varied by altering the flowrates accordingly. For example, the pumps were set to 25 ml h^{-1} flow rate to increase the residence time to 4 h. For all experiments, after the system initiated, the monitoring period was a minimum of 2 full residence times. Experiments using a 3:1 Zn:BDC ratio were repeated using both DMF and DEF to allow for comparison.

Reducing the residence time by increasing the flowrates after the initial start-up phase was also considered as a method to potentially increase the space–time yield of the product. The system was left to run with a residence time of 4 h (25 ml h^{-1} total input) as described above for 5 h. After this time, the throughput was doubled by increasing the flowrates by a factor of 2.

2.2. Characterisation

The collected solid samples were characterised by powder X-ray diffraction (PXRD), Fourier-transform infra-red spectroscopy (FTIR) and nitrogen adsorption measurements. PXRD results were collected using $Cu\ K\alpha$ ($\lambda = 1.54\text{ \AA}$) radiation source on aluminium plates. The data was analysed in order to confirm the formation and purity of MOF-5 in following two ways. A simulated PXRD pattern was generated from the single crystal diffraction data for MOF-5 reported in the literature [27] and compared with our results. Further, a Le Bail fit of X-ray powder diffraction data using General Structure Analysis System (GSAS) [29] (with initial weighting on the single crystal structure of MOF-5 [27]) reached convergence in space group $Fm\bar{3}m$ with refinement of the following 9 parameters: lattice parameters, zero point error, 6 background terms using a shifted Chebyshev function and 1 peak profile parameter. An intense and sharp Bragg peak located between 38° and $39^\circ\ 2\theta$ arose from the aluminium sample holder and was excluded from the fitting. Nitrogen adsorption–desorption measurements were performed using a Micromeritics ASAP 2420, at $-196\text{ }^\circ\text{C}$; samples were degassed by heating at $170\text{ }^\circ\text{C}$ for 24 h under vacuum.

FT-IR was carried out on an ABB MB-3000 using attenuated total reflectance (ATR) with a resolution of 4 wavenumbers and 64 scans before baseline correction and smoothing were applied to the results. Optical microscopy was completed using an Olympus BX51 at $3000\times$ zoom.

3. Results and discussion

Reaction time and temperature are known to have considerable effects upon the final product within MOF-5 synthesis, with lower temperature and slower reactions resulting in higher surface areas

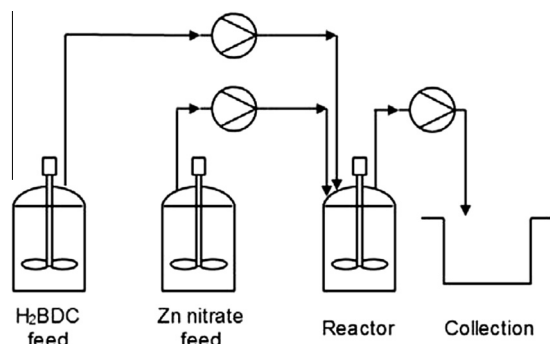


Fig. 1. Experimental layout of the continuous MOF-5 synthesis system used in this study.

than the considerably faster reactions performed at higher temperatures [28]. Kaye et al. [8] recorded the highest known Langmuir specific surface area (SSA) for MOF-5 ($3800 \text{ m}^2 \text{ g}^{-1}$) with a reaction time of 10 h at 80°C in DEF solvent. Langmuir SSAs of $>2500 \text{ m}^2 \text{ g}^{-1}$ can be formed in 2 h at 130°C as shown by Zhao et al. [30]; shorter residence times would be preferable for economically viable scale-up. Previous work by our group in analysing the formation mechanisms of MOF-5 over 0–6 h period at 110 – 140°C [28] suggested that the formation of MOF-5 occurs via a more simple pathway at 140°C . This simplified formation pathway, with a reduced number of intermediate metastable crystalline phases present, also results in the product forming in a relatively short period ($t = 2$ h) compared to many MOF-5 syntheses reported to date. Therefore, we decided to work within this region of the time–temperature (t – T) space for this study. Higher reaction temperatures are likely to reduce MOF-5 quality (e.g. low SSA) and our results below evaluate this possibility in order to recommend economical production conditions while maintaining sufficient product quality.

3.1. Understanding and optimising the process chemistry

3.1.1. Residence time requirements for MOF-5 production

Fig. 2(a) shows that samples collected from the system with 2 h residence time (140°C), over the 8 h observation window, did not produce MOF-5 at any time. When compared to the corresponding batch synthesis, MOF-5 was formed as early as 2 h at 140°C [28]. The two phases observed in Fig. 2(a) were both intermediate phases that appear to form on the way to producing MOF-5 when the residence time is insufficient to allow MOF-5 to form. This observation is consistent with recent work on batch synthesis of MOF-5 from our group and others [28,31], where it was demonstrated that the formation of MOF-5 is expected to follow a series of consecutive steps involving an intermediate solid phase and thus formation of MOF-5 can be expected to be delayed in the continuous process compared to a batch one at the same mean residence time.

When considering the residence time distribution of the continuous system, given the small vessel volume, efficient mixing and low flow rates resulting in relatively long mean residence times, it is likely that the residence time distribution follows the theoretical exponential profile for a CSTR [17]. As the formation of MOF-5 is expected to follow a series of consecutive steps, possible reasons for the lack of MOF-5 formation in the continuous system at relatively short residence times could be due to lower concentrations of reactive intermediates or intermediate solid phases at the steady state, compared to that in the batch system at the same mean residence time. One possible key intermediate is diethylamine, a

known breakdown product of the DEF solvent [32] which is essential to the MOF-5 synthesis. The constant addition of fresh DEF and removal of diethylamine in the continuous process would cause a reduction in the concentration of the amine species. Alternatively, the intermediate solid phases that form prior to the appearance of MOF-5 do not reach a concentration that is sufficient to trigger the transformation to MOF-5 when operating at 2 h residence time. Therefore the required residence time for the continuous system may need to be considerably longer than that seen in a comparable batch process. Hence, we increased the residence time of the system from 2 h to 4 h while maintaining the same temperature and precursor concentrations as stated above.

PXRD results for samples collected from the system with 4 h residence time show the presence of an intermediate phase for samples collected at times up to 3.5 h (Fig. 2(b)). The intermediate phase produced here is identical to one of the phases seen in the 2 h residence time experiment, shown in Fig. 2(a) at $t = 5.5$ h. For $t > 3.5$ h, the system produced highly pure MOF-5, which was confirmed by comparing to a simulated PXRD pattern generated from the single crystal diffraction data for MOF-5 [27] as well as by performing more rigorous analysis using a Le Bail fitting procedure (Fig. S2). The final fit gave lattice parameters of $a = b = c = 25.838$ (5) Å, which closely match with the literature values of $a = b = c = 25.669$ (3) Å [27], suggesting MOF-5 has been formed with high crystalline phase purity. A slight impurity, present in the sample taken at $t = 5$ h, was identified until the end of the observation period, however, its presence has not shown any significant reduction in surface area of MOF-5.

The theoretical yield of this system was 0.25 g h^{-1} , with actual output averaging 0.21 g h^{-1} (84% yield) at steady state, giving a space–time yield (STY) of $50 \text{ kg m}^{-3} \text{ day}^{-1}$ (see Table 1). Gas adsorption measurements for samples collected at steady state for this reactor running with excess zinc (3:1 Zn:BDC ratio) show an average Langmuir SSA of $2302 \pm 286 \text{ m}^2 \text{ g}^{-1}$ (Table 1 and Fig. S3), suggesting that good quality MOF-5 had been produced. In order to assess if any residual solvent was present, we performed further SSA measurements upon extensive solvent removal under vacuum. Such treatment did not increase the SSA significantly (Table S1), thus suggesting that our initial procedure for solvent removal was robust. Optical microscopy of the MOF-5 crystals produced confirmed the particle sizes to be generally within a range of 13–40 μm (see Fig. S4).

In order to further corroborate the presence of MOF-5, FT-IR analysis was conducted on selected samples. Fig. 3 shows FT-IR spectra from typical solid samples. Samples were taken from a DEF-based synthesis, 1% solids concentration with Zn:BDC ratio of 3:1 at times of 5 h and 6 h. Infra-red absorption for each is typical of MOF-5. The three peaks at 2978, 2939 and 2879 cm^{-1}

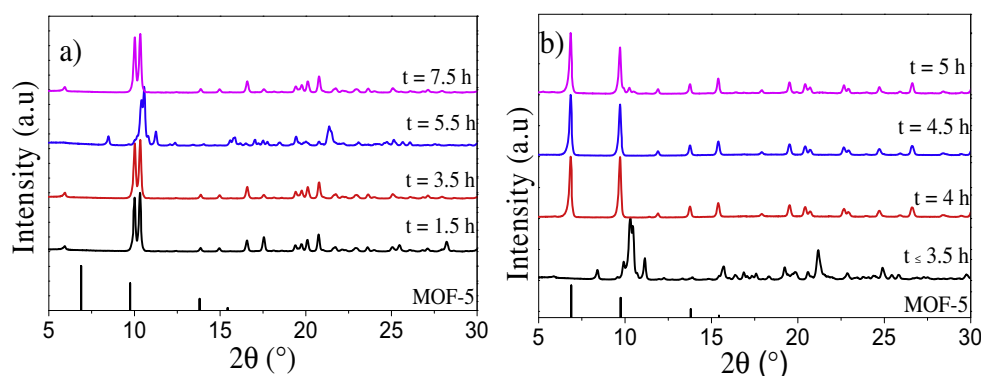


Fig. 2. PXRD results for samples collected at various time intervals with (a) 2 h and (b) 4 h residence times. The collection time for each sample was 30 min and samples were labelled as the time when collection started. Simulated PXRD result generated from single crystal data [27] is shown for comparison.

Table 1
Results of MOF-5 continuous synthesis conditions using either DMF or DEF as solvent.

Solvent	% Solids	Zn:BDC	Yield (at steady state)		STY (kg m ⁻³ day ⁻¹)	Average Langmuir SSA (m ² g ⁻¹)	Surface area production ($\times 10^6$ m ² m ⁻³ reactor day ⁻¹)
			g h ⁻¹	%			
DEF	1	3:1	0.21	84	50	2302	115
DEF	5	3:1	0.8	64	196	759	149
DEF	10	3:1	2.1	84	504	525	264
DEF	1	4:3	0.2	80	48	600	29
DEF	5	4:3	0.8	64	196	469	92
DEF	10	4:3	2.1	84	504	270	136
DMF	1	3:1	0.18	72	43	992	43
DMF	3	3:1	0.43	57	104	676	70
DMF	5	3:1	0.93	74	227	459	104

Note: 4:3 is stoichiometric, 3:1 is excess metal.

indicate the presence of amine groups from the decomposition of DEF during the reaction and are present in the wet product but not the desolvated sample. The peak present at 1650 cm⁻¹ indicates a characteristic shift in the peak location for the carboxylate group from 1610 cm⁻¹, due to interaction with the Zn₄O tetrahedra, showing the presence of bonding between organic and metal species. The peak present at 1435 cm⁻¹ also indicates deprotonated carboxylic acid bonded to the MOF-5 metal centre [33] suggesting we have bonding indicative of MOF-5, while also being generally in agreement with FT-IR spectra previously published.

The Zn:BDC ratio used within the synthesis system has a large impact upon product quality, e.g. surface area of MOF-5 produced. Therefore, we investigated a Zn:BDC ratio of 4:3 (stoichiometric), in addition to the ratio of 3:1 reported above. Both ratios produced pure phase MOF-5 according to PXRD (data not shown for 4:3 ratio sample), but the average Langmuir SSA for samples with excess zinc (3:1 Zn:BDC ratio) is 2302 m² g⁻¹, whereas the stoichiometric ratio (4:3) produced samples with surface areas of approximately 600 m² g⁻¹. When designing a process with respect to green chemistry and high atom efficiency, an excess of a feed component is not desirable [34], however in this case, the reduction in surface area means that running stoichiometric feed quantities would not be viable for further scale up.

3.1.2. Defining steady state of the MOF-5 reactor system

In order to investigate the duration of the start-up phase, multiple analyses were performed using a residence time of 4 h. The reactor products were examined using PXRD to determine whether any crystalline product had been formed and, subsequently, if MOF-5 was present. Each individual sample, therefore, showed one of three results: no crystalline material present, diffraction peaks from an intermediate phase (with or without MOF-5) were

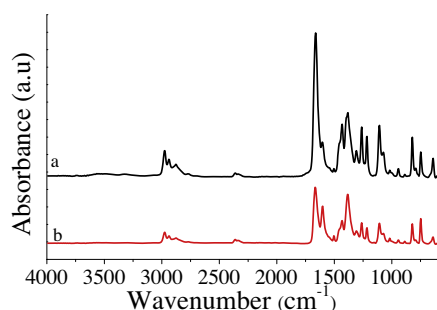


Fig. 3. FTIR results of two samples of continuously produced MOF-5. Both samples were from the same reactor run, obtained at (a) 6 h (b) 5 h.

observed or only MOF-5 was present. The fractions of each of these conditions, for 6 repeated runs as a function of the process time, are shown in Fig. 4.

A continuous MOF-5 synthesis system, operating at 4 h residence time at 140 °C was found to go through three distinct phases during the observed period (Fig. 4). At $t \geq 5.5$ h, MOF-5 was formed and the reactor appeared to be at steady state, producing high surface area samples (for 1% solids, Langmuir SSA of 2302 ± 228 m² g⁻¹) and MOF-5 was consistently the only phase observed using PXRD. Prior to this point, a start-up phase and a transient phase existed. In the start-up stage, which ran until $t = 2.5$ h, no significant solids or only low quantities of metastable crystalline intermediate phases were observed; MOF-5 was never present. The system then entered a transient region between 2.5 and 5.5 h, where both MOF-5 and intermediate phases, and mixtures thereof, were observed. The fraction of samples showing non-MOF-5 phases then diminished until the steady state region described above was reached. Through multiple repeat reactions, under identical conditions, it was possible to confirm that the metastable intermediate phases were never observed in the steady state region. This result is interesting to note for quality control purposes in continuous manufacturing of MOF-5, as an advantage over batch production.

3.2. Optimisation and process intensification

Aiming to increase the space–time yield (STY) of the MOF-5 reactor system discussed previously, we increased the concentration of the precursors to give a maximum yield of 5% and 10% MOF-5 on the basis of solid content. While greater concentrations of reactant species are likely to cause interpenetration, and reduce the surface area of the MOFs produced, in a potential scale-up

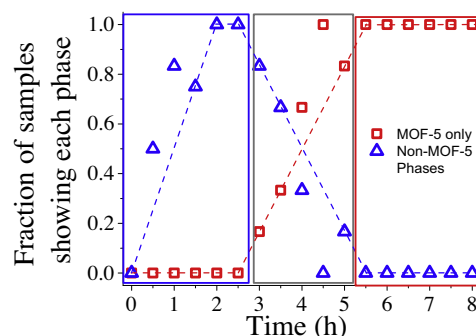


Fig. 4. Diagram of general trend for system showing start-up and MOF-5 steady state production phases. Data collected over multiple repeat runs ($n = 6$) with 4 h residence time.

where surface area per unit cost may be important, reduction in surface area may be a worthwhile compromise in order to reduce the solvent costs.

Increasing reactant concentration by a factor of 5 and 10 resulted in significantly higher STY when compared to the 1% system (see Table 1). The reactions at higher solids contents followed a formation route almost identical to the 1 wt% system, with intermediate phases detected for $t < 3.5$ h; all subsequent samples ($t \geq 3.5$ h) showed MOF-5 as the only crystalline phase formed (Fig. 5). While the output of the system was confirmed by PXRD to be MOF-5 for both 5% and 10% systems, nitrogen adsorption analyses showed that these samples had greatly reduced Langmuir SSA ($759 \text{ m}^2 \text{ g}^{-1}$ for 5%, and $525 \text{ m}^2 \text{ g}^{-1}$ for 10% systems compared to the $2302 \text{ m}^2 \text{ g}^{-1}$ recorded for the 1% solids system, Table 1). This is expected, due to the formation of an interpenetrated structure and/or the presence of amorphous impurities within the crystal structure [35].

Since increasing solids content significantly improved the STY but produced inferior quality MOF-5 (reduced SSA), a direct comparison between these systems becomes difficult. SSA is an important property of MOFs, critical to their applications and, hence, it may be more appropriate to use total surface area produced per reactor volume per time as a basis for comparing different production systems. This basis can also provide insight into the operating conditions best suited for scale up. For the MOF-5 obtained when operating at a residence time of 4 h, the total surface area production ($\times 10^6 \text{ m}^2 \text{ m}_{\text{reactor}}^{-3} \text{ day}^{-1}$) increased from 115 to 149 and 264 for 1%, 5% and 10% solids, respectively, despite the Langmuir SSA reducing from 2302 to 759 and $525 \text{ m}^2 \text{ g}^{-1}$, respectively for 1%, 5% and 10% solids (Table 1). These results highlight the potential compromise between product quality (e.g. surface area) and high yield/output.

Further attempts to increase MOF-5 production were based around the presence of three distinct output regions during the first 8 h of system operation, as shown in Fig. 4. The reactor system passed through a start-up phase and a transient phase before reaching a steady state. We investigated if a reactor allowed to establish a steady state with a 4 h residence time can be then operated at a lower residence time (2 h) in order to improve the STY.

PXRD of samples collected using a method of pre-establishing steady state showed the presence of metastable intermediate phases during $t = 1.5$ –4 h (Fig. 6). The sample collected at 4.5–5 h showed the final remnants of the transient phase, with both MOF-5 and intermediates present. Samples collected after 5 h, when the reactor was running at double the original flowrate, produced only pure-phase MOF-5, as expected. The theoretical yield of this system, at steady state, was 5 g h^{-1} , with actual output averaging 4.1 g h^{-1} (82%), at steady state, giving a STY of $984 \text{ kg m}^{-3} \text{ day}^{-1}$ an increase from $504 \text{ kg m}^{-3} \text{ day}^{-1}$ seen for the

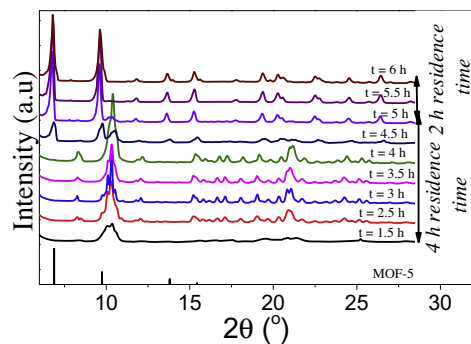


Fig. 6. PXRD showing samples collected from variable residence time MOF-5 continuous reactor run at 10% solids (M:L = 4:3). Simulated PXRD result generated from single crystal data [27] is shown for comparison.

system at a constant 4 h residence time. These results demonstrate the potential of increasing reactor output by understanding reaction mechanisms and optimisation of the process variables.

The experiments using 4 h residence time were then repeated using DMF as an alternative, cheaper solvent. While DMF generally produces MOF-5 with a lower Langmuir SSA than DEF, it is about an order of magnitude less expensive, so it is commercially available at manufacturing scale and, hence, more economically viable for a scaled-up process. Samples obtained from experiments with 4 h residence times at various solid contents were then analysed to provide a direct comparison with products obtained from DEF based reactions (Fig. 7).

Samples collected in the early phase of reactor operation (< 3 h) show the presence of the intermediate phase and no indication of the formation of MOF-5. Samples collected within the time region 3–6 h show the formation of MOF-5 only (Fig. 7 and Table 1). The crystallinity of the MOF-5 produced using DMF was reduced compared to that produced in the comparable DEF system. The crystallinity, based upon the relative intensity of Bragg peaks for MOF-5, also varied more within the DMF systems than the DEF systems. The Langmuir SSAs of the MOF-5 produced from the DMF mediated reactor were determined to investigate sample quality. MOF-5 produced using DMF showed a greatly reduced surface area with an average Langmuir SSA of $992 \pm 227 \text{ m}^2 \text{ g}^{-1}$ (Table 1) when operating at 1% solids. Upon increasing to 3 wt% and 5 wt% solids, the surface area of steady state MOF-5 produced was further reduced to $676 \pm 241 \text{ m}^2 \text{ g}^{-1}$ and $459 \pm 115 \text{ m}^2 \text{ g}^{-1}$, respectively. We were unable to produce MOF-5 successfully using DMF as the reaction solvent when operating at 10 wt% solids. As expected, from the literature, DMF based reactions produce MOF-5 with lower

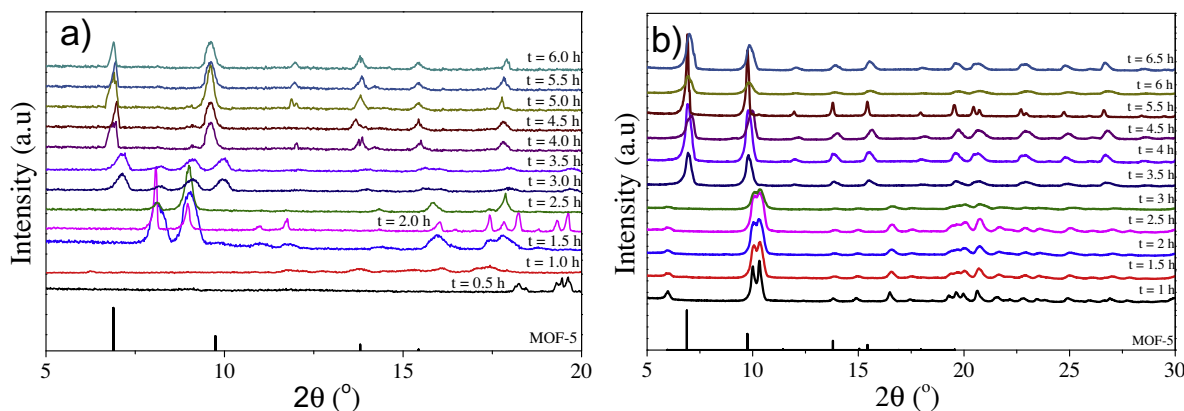


Fig. 5. PXRD results for MOF-5 continuous reactor samples produced at (a) 5% and (b) 10% solids contents and collected over $t < 6.5$ h time intervals. (M:L = 3:1, residence time = 4 h). Simulated PXRD result generated from single crystal data [27] is shown for comparison.

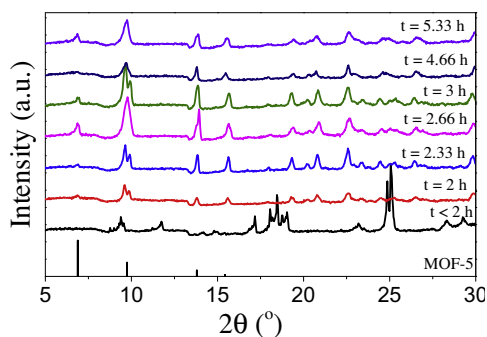


Fig. 7. PXRD results of MOF-5 continuous reactor samples prepared using DMF as a solvent with 4 h residence time collected at selected time periods ($t < 5.33$ h). Simulated PXRD result generated from single crystal data [27] is shown for comparison.

surface areas; the Langmuir SSA dropped by around 60% when switching from DEF to DMF even after sample activation at 200 °C for 24 h under vacuum prior to N₂ sorption analysis (Table S2). Comparing surface area production for both solvents (Table 1), DEF appeared to be a better choice, as expected, however, one needs to note that the price of DMF is $\sim 10\times$ lower than that of DEF, though cost savings are partially mitigated as DMF is also harder to remove from the final product, with an extra step of solvent exchange usually required to maximise available surface area [36].

4. Conclusions

We have shown here that continuous solvothermal processes for production of MOF-5 are viable and can produce high quality, high yields of MOF-5. The system was optimised by understanding the process chemistry and by exploring a number of process parameters. The number of intermediate phases seen in the continuous process was fewer than previously observed in batch processes at 140 °C. It is possible to produce a continuous reaction system for production of MOF-5, and we have optimised the system to give high purity, high surface area MOF-5. We have also shown methods for intensification allowing the STY of the system to be significantly increased to a value close to 1000 kg m⁻³ day⁻¹, which results in a reduction in surface area. While the surface area per unit mass decreases when solids concentration is increased in both the DEF and DMF based syntheses, we see an increase in the total available surface area produced per unit volume of reactor per day. As such, this may highlight the potential benefit of increasing the reactant concentrations as the specific surface area is reduced but this effect is counteracted by the production of more material within the same reaction volume.

Acknowledgements

We thank the financial support provided by the EPSRC-DTG, the Department of Chemical and Process Engineering and the Department of Pure and Applied Chemistry at the University of Strathclyde. We thank Dr. Thomas Yip for help with the PXRD analysis.

Appendix A. Supplementary data

Supplementary data associated with this article can be found, in the online version, at <http://dx.doi.org/10.1016/j.cej.2015.10.023>. Datasets associated with the figures in this article can be found online at <http://dx.doi.org/10.15129/7ce89b19-c54f-4c65-ba0c-5a7f7f267df4>.

References

- [1] S.R. Batten, N.R. Champness, X.-M. Chen, J. Garcia-Martinez, S. Kitagawa, L. Öhrström, M. O'Keeffe, M. Paik Suh, J. Reedijk, Terminology of metal-organic frameworks and coordination polymers (IUPAC recommendations 2013), *Pure Appl. Chem.* 85 (2013) 1715–1724.
- [2] J.J. Perry, J.A. Perman, M.J. Zaworotko, Design and synthesis of metal-organic frameworks using metal-organic polyhedra as supermolecular building blocks, *Chem. Soc. Rev.* 38 (2009) 1400–1417.
- [3] S. Seiffert, J. Sprakel, Physical chemistry of supramolecular polymer networks, *Chem. Soc. Rev.* 41 (2011) 909–930.
- [4] S. Hausdorf, F. Baitalow, T. Böhle, D. Rafaja, F.O.R.L. Mertens, Main-group and transition-element IRMOF homologues, *J. Am. Chem. Soc.* 132 (2010) 10978–10981.
- [5] W. Lu, Z. Wei, Z.-Y. Gu, T.-F. Liu, J. Park, J. Park, J. Tian, M. Zhang, Q. Zhang, T. Gentle Iii, M. Bosch, H.-C. Zhou, Tuning the structure and function of metal-organic frameworks via linker design, *Chem. Soc. Rev.* (2014).
- [6] A.U. Czaja, N. Trukhan, U. Muller, Industrial applications of metal-organic frameworks, *Chem. Soc. Rev.* 38 (2009) 1284–1293.
- [7] U. Mueller, M. Schubert, F. Teich, H. Puetter, K. Schierle-Arndt, J. Pastre, Metal-organic frameworks – prospective industrial applications, *J. Mater. Chem.* 16 (2006) 626–636.
- [8] S.S. Kaye, A. Dailly, O.M. Yaghi, J.R. Long, Impact of preparation and handling on the hydrogen storage properties of Zn₄O(1,4-benzenedicarboxylate)(3) (MOF-5), *J. Am. Chem. Soc.* 129 (2007) 14176–14177.
- [9] D.W. Jung, D.A. Yang, J. Kim, J. Kim, W.S. Ahn, Facile synthesis of MOF-177 by a sonochemical method using 1-methyl-2-pyrrolidinone as a solvent, *Dalton Trans.* 39 (2010) 2883–2887.
- [10] G. Blanita, O. Ardelean, D. Lupu, G. Borodi, M. Mihet, M. Coros, M. Vlassa, I. Misan, I. Coldea, G. Popeneacu, Microwave assisted synthesis of MOF-5 at atmospheric pressure, *Rev. Roum. Chim.* 56 (2011) 583–588.
- [11] M. Ma, D. Zacher, X.N. Zhang, R.A. Fischer, N. Metzler-Nolte, A method for the preparation of highly porous, nanosized crystals of isorecticular metal-organic frameworks, *Cryst. Growth Des.* 11 (2011) 185–189.
- [12] Y.Y. Liu, Z.F. Ng, E.A. Khan, H.K. Jeong, C.B. Ching, Z.P. Lai, Synthesis of continuous MOF-5 membranes on porous alpha-alumina substrates, *Microporous Mesoporous Mater.* 118 (2009) 296–301.
- [13] J.P. Li, S.J. Cheng, Q. Zhao, P.P. Long, J.X. Dong, Synthesis and hydrogen-storage behavior of metal-organic framework MOF-5, *Int. J. Hydrogen Energy* 34 (2009) 1377–1382.
- [14] D. Crawford, J. Casaban, R. Haydon, N. Giri, T. McNally, S.L. James, Synthesis by extrusion: continuous, large-scale preparation of MOFs using little or no solvent, *Chem. Sci.* 6 (2015) 1645–1649.
- [15] S.L. James, C.J. Adams, C. Bolm, D. Braga, P. Collier, T. Friscio, F. Grepioni, K.D.M. Harris, G. Hyett, W. Jones, A. Krebs, J. Mack, L. Maini, A.G. Orpen, I.P. Parkin, W. C. Shearouse, J.W. Steed, D.C. Waddell, Mechanochemistry: opportunities for new and cleaner synthesis, *Chem. Soc. Rev.* 41 (2012) 413–447.
- [16] C. McKinstry, Continuous production of two archetypal metal-organic frameworks using conventional and microwave heating (Ph.D. thesis), University of Strathclyde, 2015.
- [17] H.S. Fogler, *Elements of Chemical Reaction Engineering*, fourth ed., Prentice-Hall, 1986.
- [18] M. Faustini, J. Kim, G.-Y. Jeong, J.Y. Kim, H.R. Moon, W.-S. Ahn, D.-P. Kim, Microfluidic approach toward continuous and ultrafast synthesis of metal-organic framework crystals and hetero structures in confined microdroplets, *J. Am. Chem. Soc.* 135 (2013) 14619–14626.
- [19] E.L. Cussler, G.D. Moggridge, *Chemical Product Design*, Cambridge University Press, Cambridge, New York, 2001.
- [20] J. Harmsen, *Industrial Process Scale-up*, Elsevier, Amsterdam, Boston, 2013.
- [21] M. Mulligan, J. Rothstein, Scale-up and control of droplet production in coupled microfluidic flow-focusing geometries, *Microfluid. Nanofluid.* 13 (2012) 65–73.
- [22] P.M. Schoenecker, G.A. Belancik, B.E. Grabicka, K.S. Walton, Kinetics study and crystallization process design for scale-up of UiO-66-NH₂ synthesis, *AIChE J.* 59 (2013) 1255–1262.
- [23] M. Gimeno-Fabra, A.S. Munn, L.A. Stevens, T.C. Drage, D.M. Grant, R.J. Kashtiban, J. Sloan, E. Lester, R.I. Walton, Instant MOFs: continuous synthesis of metal-organic frameworks by rapid solvent mixing, *Chem. Commun.* 48 (2012) 10642–10644.
- [24] M. Rubio-Martinez, M.P. Batten, A. Polyzos, K.-C. Carey, J.I. Mardel, K.-S. Lim, M. R. Hill, Versatile, high quality and scalable continuous flow production of metal-organic frameworks, *Sci. Rep.* 4 (2014).
- [25] P.A. Bayliss, I.A. Ibarra, E. Perez, S. Yang, C.C. Tang, M. Poliakoff, M. Schroder, Synthesis of metal-organic frameworks by continuous flow, *Green Chem.* 16 (2014) 3796–3802.
- [26] L. D'Arras, C. Sassoie, L. Rozes, C. Sanchez, J. Marrot, S. Marre, C. Aymonier, Fast and continuous processing of a new sub-micronic lanthanide-based metal-organic framework, *New J. Chem.* 38 (2014) 1477–1483.
- [27] H. Li, M. Eddaoudi, M. O'Keeffe, O.M. Yaghi, Design and synthesis of an exceptionally stable and highly porous metal-organic framework, *Nature* 402 (1999) 276–279.
- [28] C. McKinstry, E.J. Cussen, A.J. Fletcher, S.V. Patwardhan, J. Sefcik, Effect of synthesis conditions on formation pathways of metal organic framework (MOF-5) crystals, *Cryst. Growth Des.* 13 (2013) 5481–5486.

- [29] A.C. Larson, R.B. Von Dreele, General Structure Analysis System (GSAS), Los Alamos National Laboratory Report, LAUR 86-748, 2000.
- [30] Z.X. Zhao, Z. Li, Y.S. Lin, Adsorption and diffusion of carbon dioxide on metal-organic framework (MOF-5), *Ind. Eng. Chem. Res.* 48 (2009) 10015–10020.
- [31] J. Kim, M.R. Dolgos, B.J. Lear, Isolation and chemical transformations involving a reactive intermediate of MOF-5, *Cryst. Growth Des.* 15 (2015) 4781–4786.
- [32] S.W. Hausdorf, Proton and water activity-controlled structure formation in zinc carboxylate-based Metal Organic Frameworks, *J. Phys. Chem. A* 112 (2008) 7567–7576.
- [33] D.P.D. Saha, S.G. Deng, Z.G. Yang, Hydrogen adsorption on metal-organic framework (MOF-5) synthesized by DMF approach, *J. Porous Mater.* 16 (2009) 141–149.
- [34] R.A. Sheldon, Why green chemistry and sustainability of resources are essential to our future, *J. Environ. Monit.* 10 (2008) 406–407.
- [35] J. Hafizovic, M. Bjorgen, U. Olsbye, P.D.C. Dietzel, S. Bordiga, C. Prestipino, C. Lamberti, K.P. Lillerud, The inconsistency in adsorption properties and powder XRD data of MOF-5 is rationalized by framework interpenetration and the presence of organic and inorganic species in the nanocavities, *J. Am. Chem. Soc.* 129 (2007) 3612–3620.
- [36] L. Zhang, Y.H. Hu, Desorption of dimethylformamide from Zn(4)O(C(8)H(4)O(4))(3) framework, *Appl. Surf. Sci.* 257 (2011) 3392–3398.